Harmonic Elastography Through Time-of-Flight Calculations

Murthy N. Guddati
NC State University
Raleigh, NC, USA
mnguddat@ncsu.edu

***Abstract*— This work addresses the IUS challenge focused on assessing the accuracy of various methods in providing elastography images of soft tissue using shear wave elastography (SWE) data, specifically from harmonic excitation. The challenge is not necessarily aimed at developing new methodologies but applying existing (or new) methodologies to assess their accuracy. In this spirit, we illustrate that simple time-of-flight calculations can provide useful first-order-approximate reconstruction of the underlying structure.**

Keywords— elastography challenge

I. Introduction

For the harmonic challenge, IQ data is provided over a single plane of measurement for three separate phantoms, and the objective is to reconstruct the elasticity map for each of the phantoms. The first and third phantoms have inclusions, while the second is a homogeneous phantom. The geometry of the experimental setup is not provided, but the frequencies of excitation are provided, which include 6 different frequencies, 100 Hz to 200 Hz, with a frequency increment of 20 Hz. The data is provided on a grid of 0.431 mm spatial resolution and 1 ms temporal resolution.

II. Methods

Complete geometric and excitation details would be necessary, and sufficient, to perform robust full waveform inversion (FWI, e.g. [1]) in the frequency domain which has the potential to result in accurate images with sub wavelength resolution. However the provided information is limited in this regard and challenged us to build the image of shear wave velocity without these details. Fortunately, visual observation of the particle velocity data for all three phantoms indicate that wave packets are propagating largely in the x direction, albeit back and forth as expected. The response also included some upward and downward propagating waves. The observation of horizontal packet-like wave propagation led to the hypothesis that simple time-of-flight (ToF) calculations with proper attention to pertinent details can lead to reasonable elastographs. This is the approach that we took in this effort. The first step is to convert the IQ data into vertical particle velocity distribution in the measurement plane as a function of time, using standard correlation approaches. The particle velocity is then smoothed using moving average filter in the z direction. The resulting data is then processed for each z independently of each other (an example x-t representation of the particle velocity for a specific z is shown in Fig. 1; this is the data that is processed for building the shear velocity map for that particular z) . Such an approach, while primitive and ignores 2D scattering effects, is somewhat standard in many approaches. We employed such an approximation keeping in mind that the other approximations made in the remaining steps, e.g. directional filtering discussed below, will be of similar order. The steps entail directional and other filtering followed by time-of-flight calculations (somewhat unconventional given the harmonic data). These are illustrated leading to the remainder of the section.

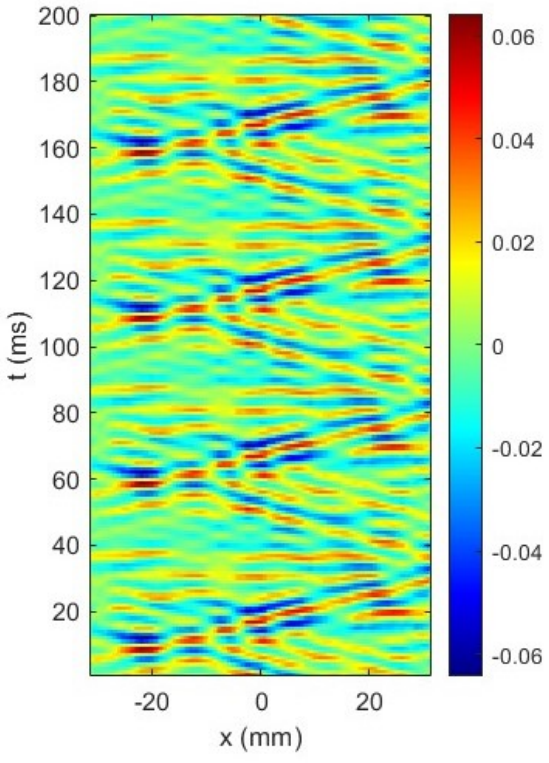

Fig 1. Typical x-t plot of particle velocity illustrating both leftward and rightward propagating waves as well as resonant modes and other spurious artifacts.

The work is funded in part by the National Institute of Health grant R01 HL145268, National Science Foundation grant DMS-2111234.

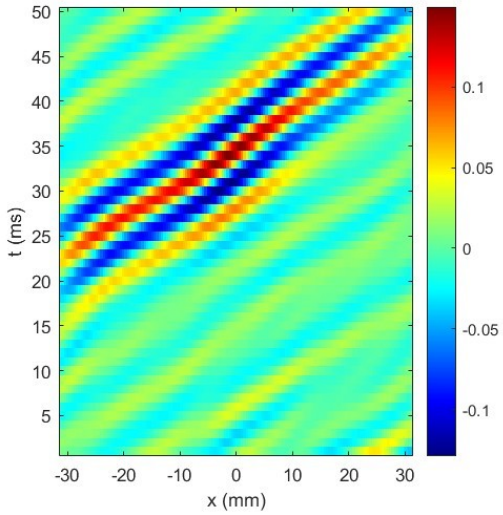

Fig 2. Right propagating waves highlighted after filtering out the left propagative waves as well as resonant and other artifacts that appear in the full wavefield shown in Fig, 1. Note that only a single cycle of Fig,1 is shown here.

A. Directional Filtering

Examining the example *x-t* representation of particle velocity in Fig. 1, we note that the motion includes left and right propagating waves, resonant vibrations as well as other artifacts that appear as very slow and very fast propagating waves. Considering this, we first isolate rightward propagating waves by transforming the particle velocity to frequency-wavenumber (*f-k*) domain, followed by muting negative phase velocities (second and fourth quadrants in *f-k* domain). Additional windowing is performed to eliminate the upward and downward propagating waves as well. In addition, any resonant modes are removed by only including the response associated with the provided excitation frequencies. These additional processing steps lead to further highlighting of the

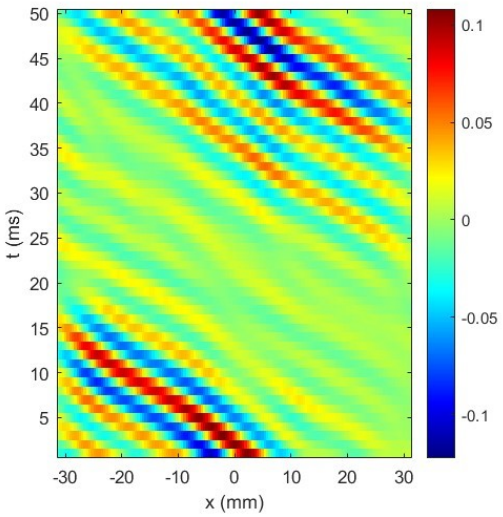

Fig 3. Left propagating waves highlighted after filtering out the right propagative waves as well as resonant and other artifacts.

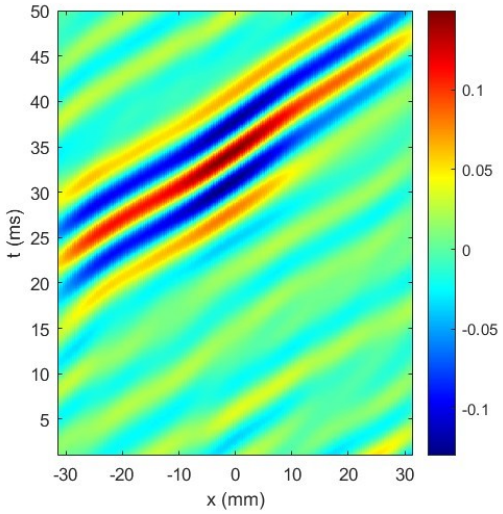

Fig 4. Spline smoothing of the directionally filtered wave associated with dominant propagation in Fig. 2.

right propagating waves (see Fig. 2).

B. Left or Right Progagating Waves?

The above filtering is also performed to isolate leftward propagating waves as well (see Fig. 3). Dominant propagation direction is then chosen by comparing the respective energies (least-squares norms) of the signal across the entire depth. The next two steps are applied to the filtered particle velocities highlighting the dominant propagation direction.

C. Time-of-Flight Calculations

For the wave packets, the ToF approach is applied not to the peak locations of response, but to the zero locations next to the peaks. This detail is particularly important given the coarse temporal sampling necessitating interpolation; the resulting error would be less in locating the zeros as opposed to the peaks. Spline interpolation is performed given the coarse temporal resolution of the data; apparently more natural Fourier based interpolation did not work as well, potentially due to the noise in the data.

D. Resonctructing the Shear Wave Velociy Map

For each *z* line, and at each *x* location, ToF is computed in the x neighborhood of seven points. Least-squares averaged slope of the local ToF curve is computed to obtain the local slowness, which is then converted to result in an image of the shear wave velocity.

III. Results and Discussion

The resulting images for the three phantoms are shown in Fig. 5 for the three phantoms, along with the regions of interest related to inclusions (if any). sharpness of the images can be improved by obtaining the particle velocity with high temporal resolution associated with higher frequency excitation, leading to lower wavelengths and higher resolution. In addition, or even alternatively, details of global geometry and excitation would enable the application of FWI, which is a focus of our

research group [1]. The current images would serve as an excellent starting points for such FWI. Nevertheless, independently of FWI, the images from ToF calculation are expected to be a reasonable first order approximations of the real shear wave velocity maps.

REFERENCE

[1] A. Elmeliegy, M.N. Guddati (2023), "Correlation-based full-waveform shear wave elastography," Physics in Medicine & Biology, vol. 68, 115001.

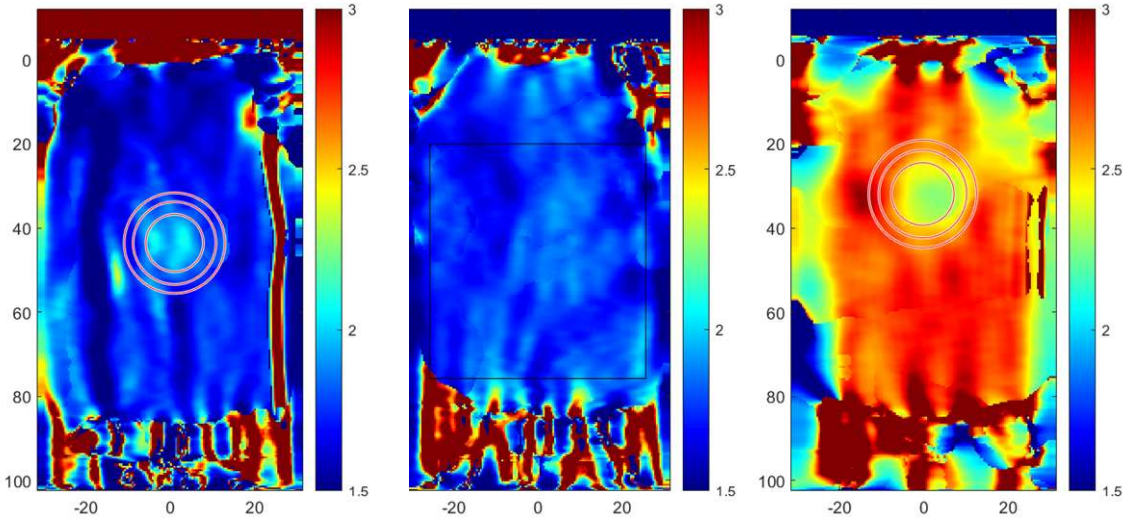

Fig 5. The resulting reconstructions from the employed ad hoc approach. The left is for phantom 1, middle is for phantom 2 and the right is for phantom 3. The color scale represents shear wave velocity in *m/s*. The circles in the left and right figures are the regions of interest highlighted in the challenge, representing the location of the inclusions. The images are understandably coarse and are expected to be improved significantly with the help of techniques such as full waveform inversion.